Adsorption (2015) 21:523–531
DOI 10.1007/s10450-015-9691-7

Development of a system of natural gas storage governed by simultaneous processes of adsorption–desorption

Rodrigo G. Martins[1] · Deivson C. S. Sales[1] · Nelson M. Lima Filho[1] · Cesar A. M. Abreu[1]

Received: 24 April 2015 / Revised: 20 July 2015 / Accepted: 10 September 2015 / Published online: 19 September 2015

Abstract A system for natural gas storage was developed where energy effects involved in adsorption and desorption were combined through two concentric cylinders containing equal masses of activated carbon. The storage operating cycle was performed using methane feeding (compression/adsorption) in the internal cylinder, while simultaneously methane discharging (decompression/desorption) in the external cylinder. The charge and discharge operations were evaluated using the barometric technique at 298 K under storage pressures of 10, 30 and 60 bar, with flow rates of 1.14×10^{-3}, 5.13×10^{-3} and 9.09×10^{-3} m^3/min. The coaxial storage system provided faster pressure and temperature evolution toward equilibrium. A 50 % increase in the mass of gas stored under 60 bar was obtained when compared with the single storage tank.

Keywords Storage · Natural gas adsorption · Desorption · Coaxial system

List of symbols

Variables

$d_{c,int}$	Internal diameter of storage tank (m)
h_c	Height of storage tank (m)
m_{AC}	Mass of activated carbon (kg)
$n_{ads\ CH4}$	Number of methane molecules adsorbed (mol)
$n_{f,CH4}$	Number of moles of methane fed (mol)
$n_{micro,CH4}$	Number of moles trapped in the micropores (mol)
n_{ext}	Number of moles compressed in the mesopores and macropores, and in the free space of the reservoir (mol)
q^*_{CH4}	Adsorbed methane at equilibrium
q^{IC}_{CH4}, q^{ES}_{CH4}, q^{ST}_{CH4}	Amount of adsorbed methane in the internal cylinder, external cylinder, single tank (kg/kg)
M	Molar mass of the gas (kg/mol)
P	Pressure (bar)
Q	Flow rate (m^3/min)
$Q^{IC}_{V/V}$, $Q^{ES}_{V/V}$, $Q^{ST}_{V/V}$	Volumetric storage capacity in the internal cylinder, external cylinder, single tank (m^3/m^3)
T	Temperature (K)
V_S	Specific volume of the adsorbent (m^3/kg)
V_P	Specific pore volume (m^3/kg)
V_{micro}	Specific volume of the micropores (m^3/kg)
$V_{micro,Q}$	Specific volume of gas filled at the micropores (m^3/kg)
Z	Compressibility factor

Greeck letters

ρ_{pc}	Packing density (kg/m^3)
ε	Porosity of the activated carbon
$\varepsilon\underline{s}$	Storage efficiency

✉ Cesar A. M. Abreu
cesar@ufpe.br; deivson.cesar@yahoo.com.br

[1] Department of Chemical Engineering, Federal University of Pernambuco, Avenida Prof. Artur de Sá s/n, Recife, PE 50740-520, Brazil

1 Introduction

The increasing availability of natural gas (NG) associated with its different forms of consumption has in turn increased its impact on energy matters. NG is a natural resource for industries, households and automotive vehicles. In the case of industrial use, it sometimes must be transported to locations where there is no pipeline system. For this, NG has to be transported and stored in special high-pressure tanks, normally in the range of 200–250 bar.

Storage and transport operations by adsorption on porous materials may be performed under lower pressures. NG storage technology by adsorption (ANG) on activated carbon under moderate pressures (35–40 bar) is the main alternative to compressed NG, reducing the processing costs and increasing storage capacity (Lozano-Castelló et al. 2002b). Due to their large superficial area, packing density and high micropore volume, activated carbons have the highest adsorption capacity of the other absorbents, for NG (Wegrzyn and Gurevich 1996; Biloé et al. 2001; Basumatary et al. 2005). Recently, novel materials have been developed that offer similar or higher adsorption capacities for gas storage (Mason et al. 2014; Gadipelli and Guo 2015). Different NG charge and discharge methods for storage systems have been proposed to evaluate the performance and corresponding heat effects (Do, 1995; Mota et al. 1995; Chang and Talu 1996; Pupier et al. 2005; Yang et al. 2005; Yahia and Ouederni 2012). Evidence of heat release during gas loading on the system are due to the effects of compression and adsorption. In consequence, the increase in temperature lowers the storage capacity of the reservoir. During discharge of the stored gas, decompression and desorption effects are involved and heat absorption occurs. Thus, the temperature in the vessel decreases making it difficult to release the gas. In order to improve the efficiency of the storage systems using adsorption, several methods have been studied, including evaluations of reservoir configuration (Santos et al. 2009; Vasiliev et al. 2000; Prajwal and Ayappa 2014) and application of charge and discharge cycles (Mota 1999; Bastos-Neto et al. 2005; Hirata et al. 2009; Walton and LeVan 2006; Stritih and Bombač, 2014).

The present work proposes the use of a new gas storage system where two coaxial cylinders are filled with an equal mass of activated carbon, in order to improve the NG storage capacity using the ANG process. Simultaneous operations of charge and discharge were performed involving the combination of thermal effects due to adsorption and desorption. A methane storage study compares the coaxial system with a traditional system (single storage cylinder) based on the temperature and pressure evolutions in the charging and discharging steps.

2 Materials and methods

2.1 Gases and adsorbent

Two gases, methane (99.5 % purity, Praxair, Br) for storage, and helium (99.9 % purity, Praxair, Br) to determine the total accessible volume of the storage system, were used in contact with activated carbon ($m_{AC} = 1.32 \times 10^{-1}$ kg, $d_p = 0.68 \times 10^{-3}$ m; Nuchar, NG MeadWestvaco, USA), obtained from wood and chemically activated. The textural characteristics of activated carbon (NG Nuchar-MedWest vacuum, specific surface area, pore volume, micropore volume, mean pore diameter) were evaluated by the BET-N_2 method (ASAP 2010).

2.2 Semi-pilot unit

Experimental evaluations for methane storage were conducted in a semi-pilot plant (Fig. 1). The coaxial storage tank is shown in Fig. 2. It consists of two concentric cylinders where the wall of the external cylinder is thermally isolated. The tanks have the same volume and both contain the same amount of activated carbon.

2.3 Experimental procedure

The experimental evaluations consisted of cyclic methane storage operations involving charging and discharging of the gas carried out under non-isothermal conditions. First, methane was fed into the internal storage cylinder at the rates of 1.14×10^{-3}, 5.13×10^{-3}, 9.09×10^{-3} m^3/min, starting at 0.1 bar and going until the desired loading pressure (10, 60 bar) had been reached. Then the gas supply was interrupted, until the pressure and temperature reached equilibrium. In the second step, methane was fed into the external cylinder while the accumulated gas in the internal cylinder was simultaneously discharged at the same rate as the methane flow. The operation continued until the pressure within the external cylinder reached the charge pressure value while the external cylinder was depleted.

2.4 System characteristics and experimental evaluation

The volumetric capacity (V/V) of the gas was calculated using Eq. 1 (Matranga et al. 1992), where the first term represents the gas stored by adsorption and the second term represents the gas stored by compression.

$$Q_{V/V} = \frac{q^*_{CH4}\rho_{pc}RT_0}{MP_0} + \left(\frac{\varepsilon_S}{Z}\right)\left(\frac{P}{P_0}\right)\left(\frac{T_0}{T}\right) \quad (1)$$

The values of P_0 e T_0 are given in the STP. M (kg/mol) is the molar mass of the gas and ρ_{pc} the packing density. Z

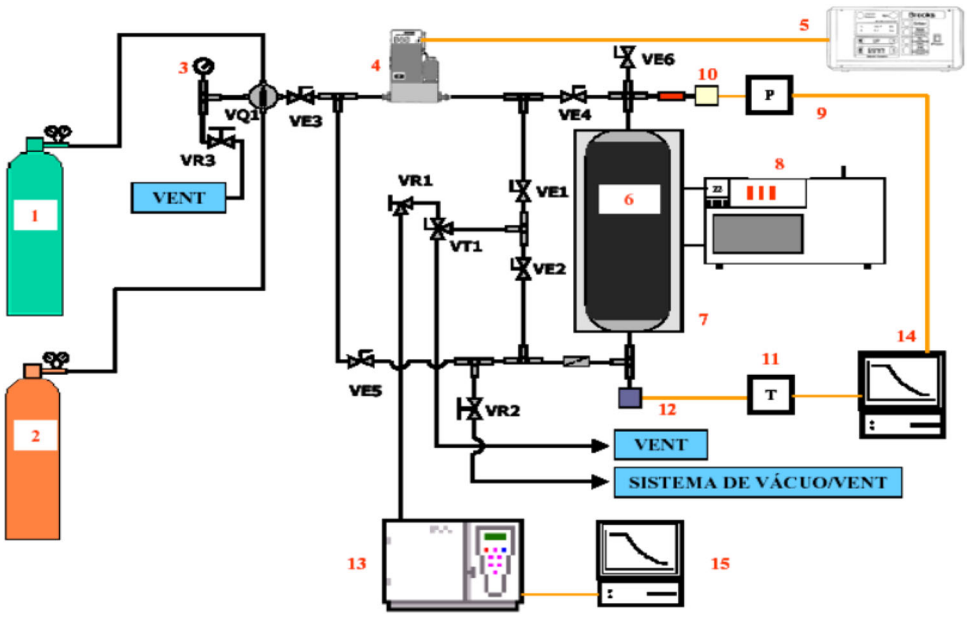

Fig. 1 Diagram of the storage unit: (*1*) helium cylinder, (*2*) methane cylinder, (*3*) manometer, (*4*) high pressure mass flow meter and controller, (*5*) flow meter controller, (*6*) storage tank ($d_{c,int} = 4.6 \times 10^{-2}$ m, internal diameter; $h_c = 35.0 \times 10^{-2}$ m, height), (*7*) heating jacket, (*8*) thermostatic bath, (*9*) manometer, (*10*) pressure transducer, (*11*) thermometer, (*12*) thermocouple, (*13*) computer

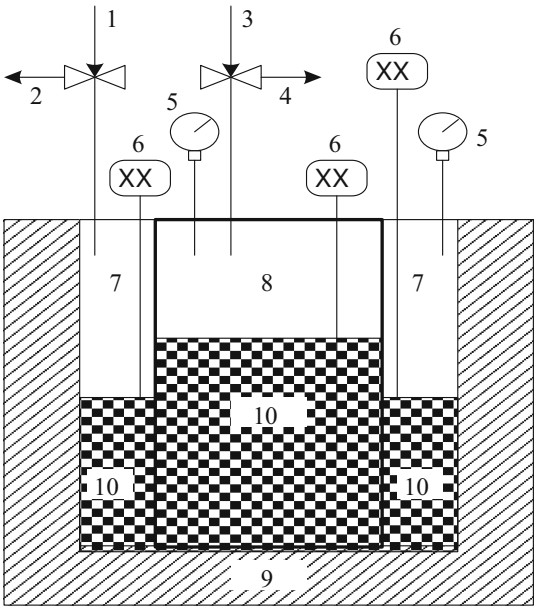

Fig. 2 Coaxial system for storage of natural gas by compression and adsorption. (*1*, *3*) feed, (*2*, *4*) discharge, (*5*) transductors, (*6*) thermocouples, (*7*) external cylinder, (*8*) internal cylinder, (*9*) insulation, (*10*) fixed beds of activated carbon

is the compressibility factor at T and P, calculated using the Peng-Robinson's equation (Reid et al. 1987). ε_s the storage efficiency of the system was obtained as follows (Eq. 2):

$$\varepsilon_S = \varepsilon + \left[V_p - \left(V_{micro} - V_{micro,Q}\right)\right]\rho_{pc} \quad (2)$$

where $V_{micro,Q}$ is the specific volume of gas filling the micropores.

2.5 Quantification of adsorbed methane

The adsorbed methane on activated carbon at equilibrium q^*_{CH4} was calculated as:

$$q^*_{CH4} = n_{ads,CH4}/m_{AC} \quad (3)$$

where m_{AC} was the mass of activated carbon in the storage tank and $n_{ads\ CH4}$ the number of moles of methane adsorbed given by Eq. 4.

$$n_{ads,CH4} = n_{f,CH4} - n_{micro,CH4} - n_{ext} \quad (4)$$

$n_{f,CH4}$ and $n_{micro,CH4}$ were the number of moles of methane fed into the system and the number of moles trapped in the micropores of the activated carbon, respectively. The number of moles compressed in the mesopores and macropores, and in the free space of the reservoir was n_{ext}. This was measured by charging the system with helium, considering that this gas is not adsorbed on activated carbon.

3 Results and discussion

3.1 Characteristics of adsorbent

The textural characteristics of the adsorbent (NG Nuchar, Med West Vacuum, USA) evaluated by the BET-N_2 method are listed in Table 1. The activated carbon had a large specific surface area and a high pore volume, which favors the adsorption and accumulation of methane.

$$\varepsilon = 1 - \rho_{pc}(V_S - V_P) \quad (5)$$

Table 1 Textural characteristics of activated carbon (NG Nuchar, Med West Vacuum USA)

Superficial area BET (m^2/g)	1634
Pore volume × 10^6(m^3/g)	1.04
Micropore volume × 10^6(m^3/g)	0.52
Pore diameter (Å)	25.47

where V_S is the specific volume of the adsorbent and V_P specific pore volume. ρ_{pc} is calculated as 308.64 kg/m^3.

3.2 Experimental evolutions

The methane storage process was evaluated through the measurement of the pressure and temperature evolutions obtained during the charge and discharge operations carried out in the internal and external reservoirs of the coaxial system. The pressure evolutions in the internal reservoir (Figs. 3, 4), involving compression and adsorption, reached the charge pressures (10, 60 bar) at 1.5 and 3.5 min, respectively, operating at a flow rate of 1.14×10^{-3} m^3/min. After 5 min, the equilibrium pressures of 8.5 and 55 bar were reached.

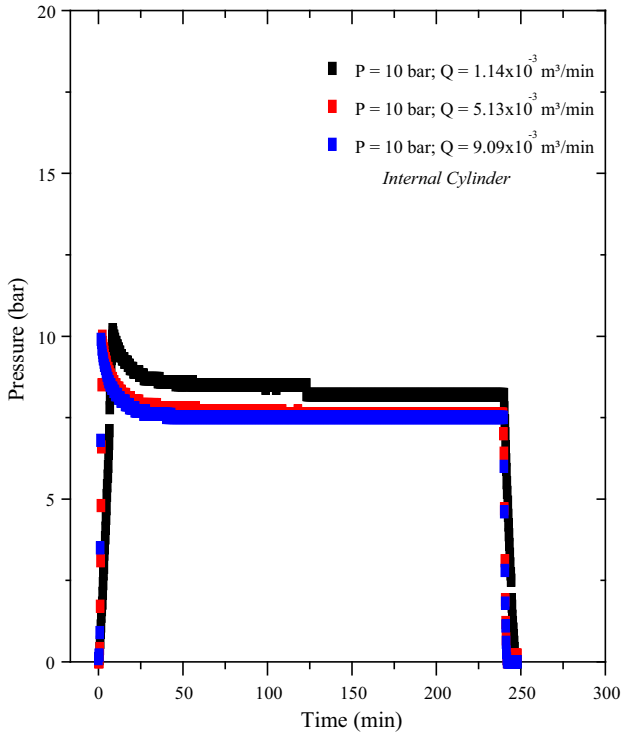

Fig. 3 Evolution of storage pressure. Influence of feed flow rate. *Conditions* coaxial system, methane, internal cylinder, charge pressure, 10 bar; mAC =1.32 × 10^{-1} kg

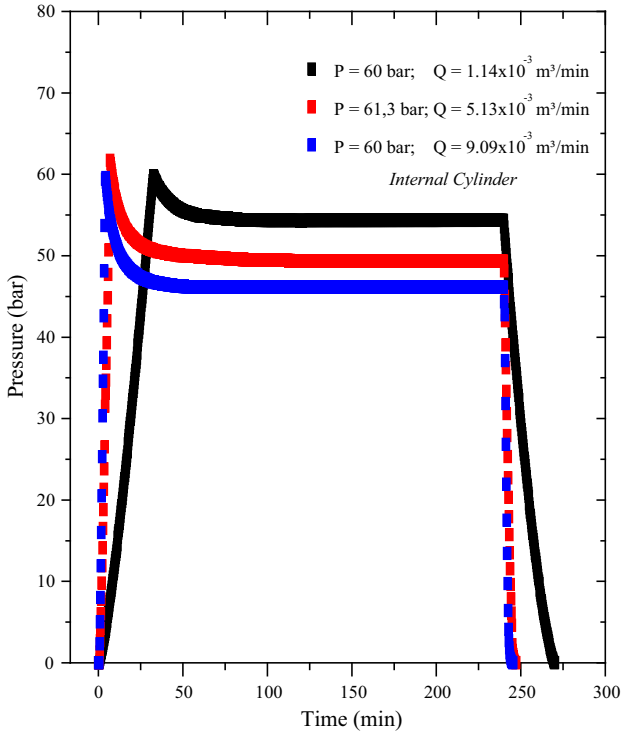

Fig. 4 Evolution of storage pressure. Influence of feed flow rate. *Conditions*: Coaxial system, methane, internal cylinder, charge pressure, 60 bar; $mAC = 1.32 \times 10^{-1}$ kg

The discharge step involving decompression and desorption, carried out from after the equilibrium pressure (55 bar) until 0.5 bar, was performed in 2 min with the discharge flow rate at 1.14×10^{-3} m^3/min.

Similar pressure evolutions were observed in the storage operations carried out in the external reservoir (Figs. 5, 6). The charge and discharge times were near those obtained in the operations of the internal reservoir, and the equilibrium pressure was 10 bar and 60 bar, respectively, with the three feeding flows.

The temperature evolutions measured during the process steps (Figs. 7, 8, 9, 10) indicate the effects of the energy released or absorbed due to the adsorption, desorption and compression/decompression processes. These energy effects were observed through the temperature evolutions measured in the internal reservoir (Figs. 7, 8) and in the external reservoir (Figs. 9, 10): higher temperatures (48 °C) were reached for operations with higher charge pressure (60 bar) and feed flow rate (9.09×10^{-3} m^3/min) during the charge step in the internal reservoir. Under the same conditions (internal reservoir, 60 bar, 9.09×10^{-3} m^3/min) a temperature below 0 °C was reached during the discharge step.

In all operations performed in the internal and external tanks, the equilibrium temperature was 24–26 °C. This was close to the methane feed temperature range, indicating the

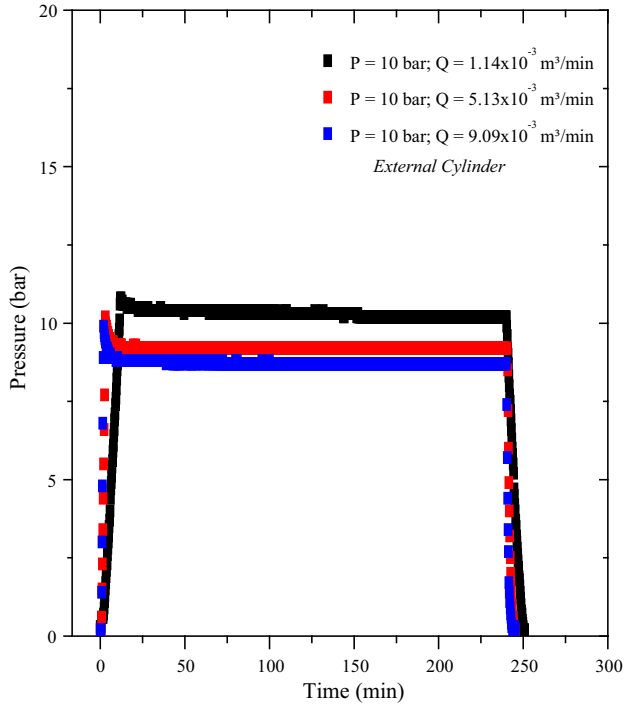

Fig. 5 Evolution of storage pressure. Influence of feed flow rate. *Conditions* coaxial system, methane, external cylinder, charge pressure, 10 bar; $m_{AC} = 1.32 \times 10^{-1}$ kg

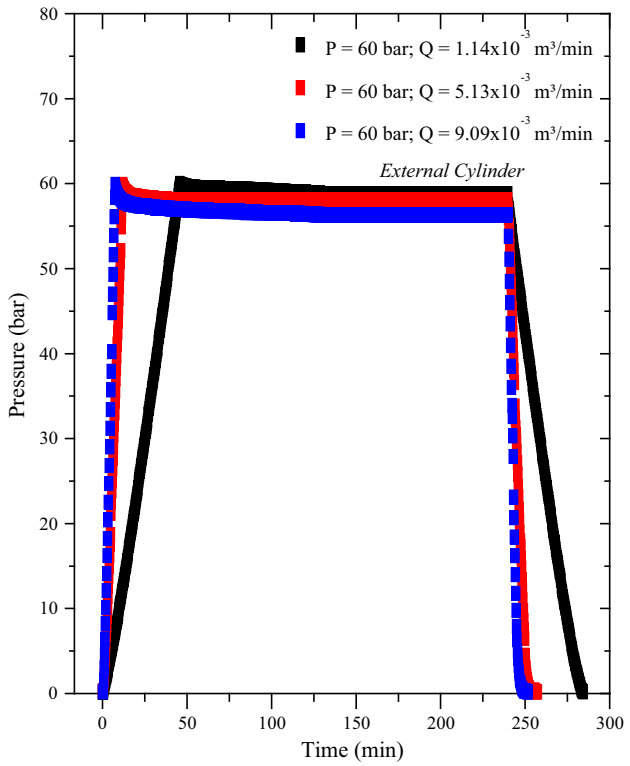

Fig. 6 Evolution of storage pressure. Influence of feed flow rate. *Conditions* coaxial system, methane, external cylinder, charge pressure, 60 bar; $m_{AC} = 1.32 \times 10^{-1}$ kg

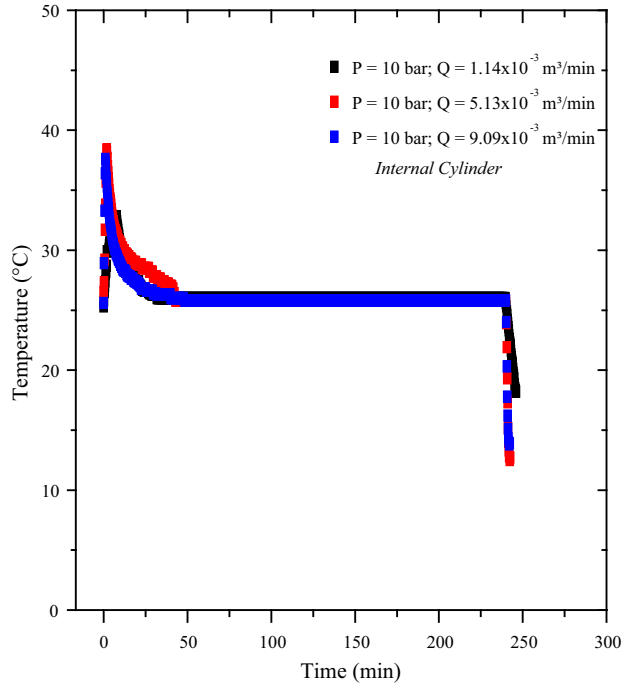

Fig. 7 Evolution of temperature. Influence of feed flow rate. *Conditions* coaxial system, methane, internal cylinder, charge pressure, 10 bar; $m_{AC} = 1.32 \times 10^{-1}$ kg

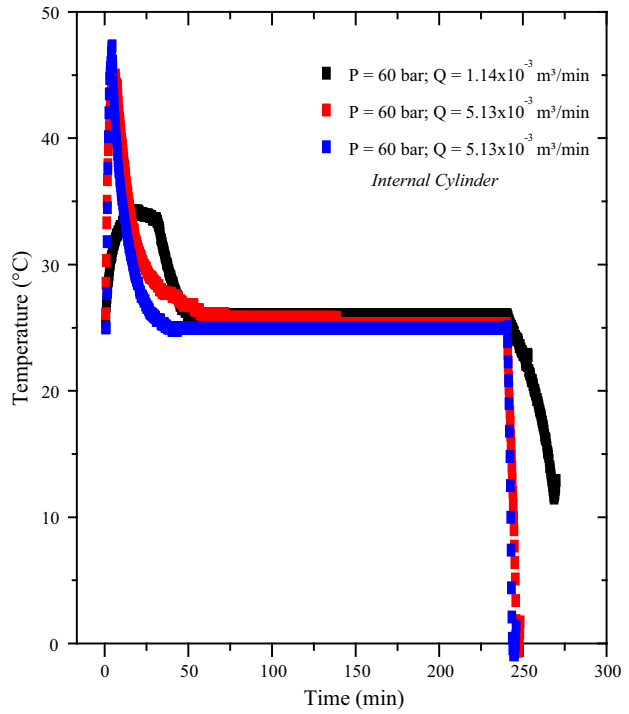

Fig. 8 Evolution of temperature. Influence of feed flow rate. *Conditions* coaxial system, methane, internal cylinder, charge pressure, 60 bar; $m_{AC} = 1.32 \times 10^{-1}$ kg

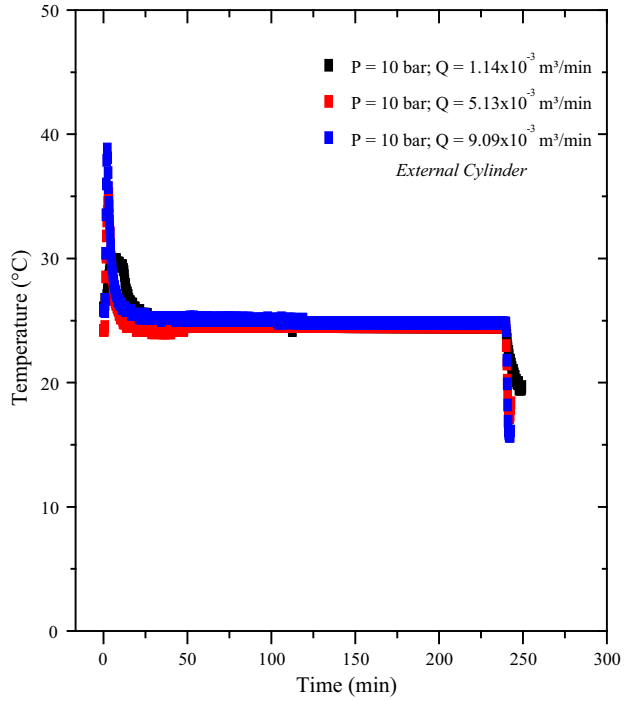

Fig. 9 Evolution of temperature. Influence of feed flow rate. *Conditions* coaxial system, methane, external cylinder, charge pressure, 10 bar; $m_{AC} = 1.32 \times 10^{-1}$ kg

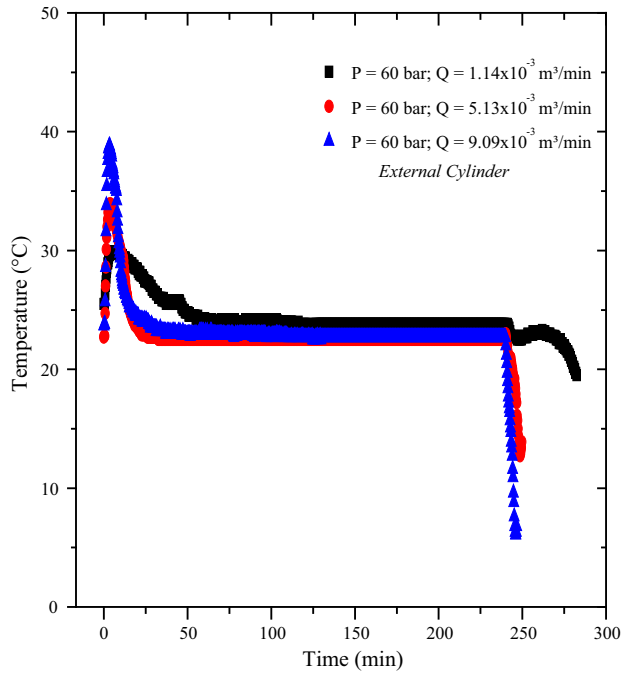

Fig. 10 Evolution of temperature. Influence of feed flow rate. *Conditions* coaxial system, methane, internal cylinder, charge pressure, 60 bar; $m_{AC} = 1.32 \times 10^{-1}$ kg

occurrence of systematic thermal exchange between the storage reservoirs. The released heat during the gas feeding in the internal reservoir, mainly due to the exothermic adsorption, was removed from this reservoir via transfer through the common wall between the concentric reservoirs. This was also promoted by the heat absorption occurring during the gas discharge in the external reservoir, mainly due to the its desorption. The gas storage was more pronounced in the internal reservoir in the charge step, because a lower temperature had been reached, while more gas was removed from the external reservoir in the discharge step, because a higher temperature had been reached.

3.3 Comparison of the ANG storage systems

Storage operations carried out in the coaxial system were compared to those carried out on a single tank system. Equal activated carbon masses were used in the single storage tank and in each reservoir of the coaxial system. Figures 11 and 12 show that the equilibrium pressures were achieved faster in the coaxial system operations. The equilibrium pressures obtained in the internal reservoir were lower than those obtained in traditional systems, and this result indicated a higher methane adsorption. The charging operation in the external reservoir required more time to reach the same pressure obtained in the traditional system, probably due to the high adsorption capacity developed in the coaxial system with more gas being fed.

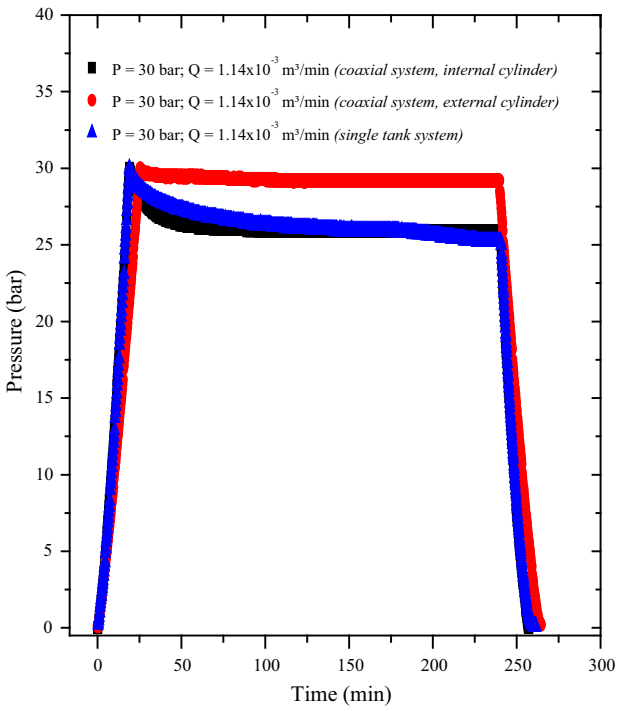

Fig. 11 Comparative evolutions of storage pressure. *Conditions* coaxial system, methane, charge pressure, 30 bar; 1.14 × 10–3 m^3 min^{-1}; $m_{AC} = 1.32 \times 10^{-1}$ kg

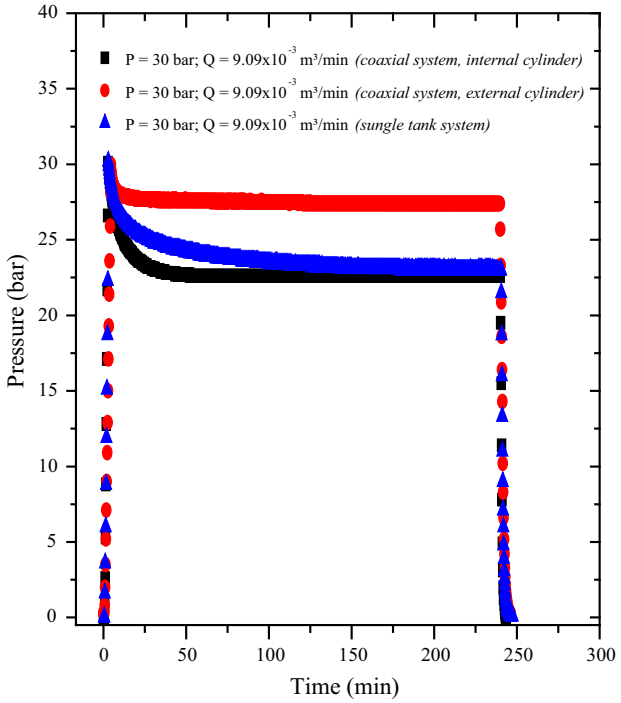

Fig. 12 Comparative evolutions of storage pressure. *Conditions* coaxial system, methane, charge pressure, 30 bar; 9.09 × 10–3 m^3 min^{-1}; $m_{AC} = 1.32 \times 10^{-1}$ kg

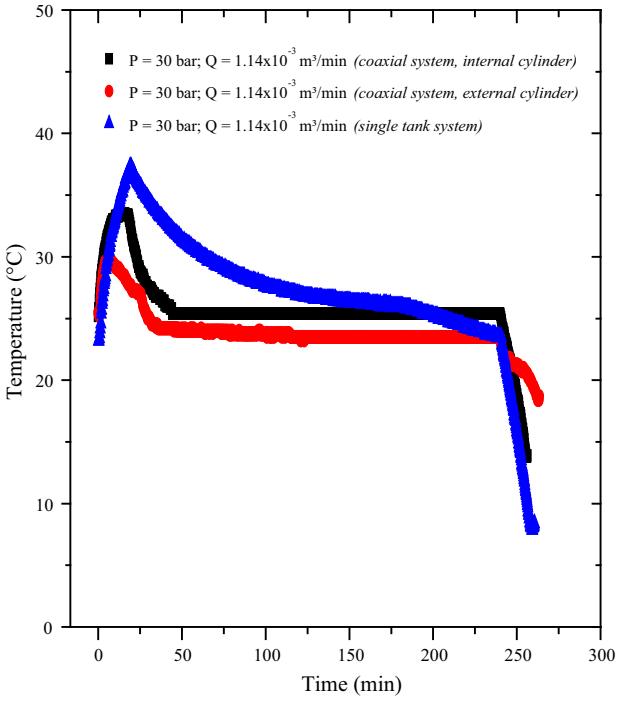

Fig. 13 Comparative evolutions of temperature. *Conditions* coaxial system, methane, charge pressure, 30 bar; 1.14 L/min; $m_{AC} = 1.32 \times 10^{-1}$ kg

Similar behavior was observed in the discharge operation, where a greater volume of gas was desorbed and removed.

The temperature evolutions in the traditional and coaxial systems for the charge pressure of 30 bar, with the flow rates of 1.14×10^{-3} m/min and 9.09×10^{-3} m^3/min, are shown in Figs. 13 and 14. In the coaxial system, the equilibrium temperature was reached faster than in the traditional system, confirming the significance of the heat exchange between the concentric cylinders.

As to methane storage, performed in the traditional and coaxial systems containing activated carbon, the concentration of adsorbed methane was calculated under different operating conditions, in the adsorption equilibrium. In Table 2, the absorbed amounts (q^{IC}_{CH4}, q^{ES}_{CH4}, q^{ST}_{CH4}; *internal, external, single*) are listed according to the flow rate, and charge pressure. Results concerning the volumetric storage capacity of the traditional and coaxial systems ($Q^{IC}_{V/V}$, $Q^{ES}_{V/V}$, $Q^{ST}_{V/V}$; *internal, external, single*) are presented in Table 3. Comparisons between the two systems are expressed in percentage by weight and by volume, respectively.

The amount of gas adsorbed was dependent on the charge pressure and was practically independent of the feed flow rate. Even with reservoirs containing an equal mass of activated carbon, the methane-adsorbed amount was higher in the external reservoir. In comparison with the traditional

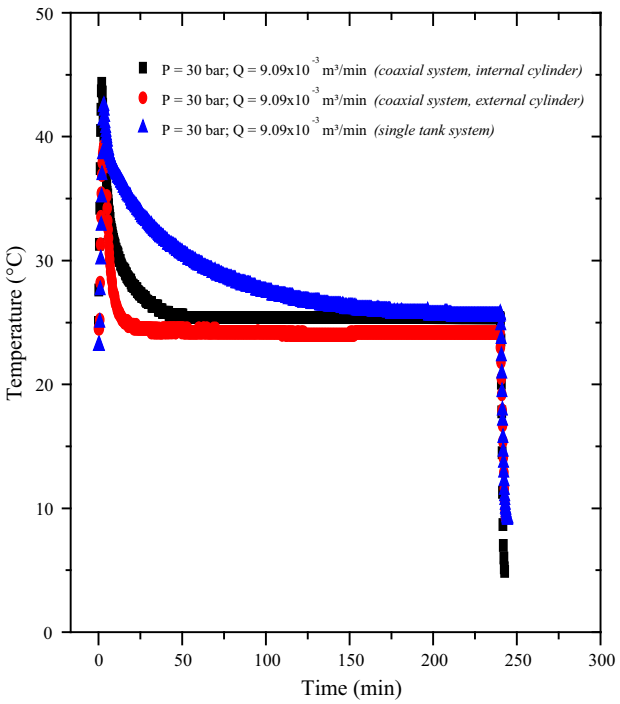

Fig. 14 Comparative evolutions of temperature. *Conditions* coaxial system, methane, charge pressure, 30 bar; 9.09 L/min; $m_{AC} = 1.32 \times 10^{-1}$ kg

Tabel 2 Comparative evaluation for the storage systems

Flow rate $\times 10^3$ (m^3/min)	Internal cylinder		External cylinder		Single tank		Mass storage increase in the coaxial system	
	P (bar)	$q_{CH4}^{IC} \times 10^2$ (kg/kg)	P(bar)	$q_{CH4}^{CE} \times 10^2$ (kg/kg)	P (bar)	$q_{CH4}^{ST} \times 10^2$ (kg/kg)	$\left(\frac{q_{CH4}^{CI}}{q_{CH4}^{ST}} - 1\right)$ *Internal (%)*	$\left(\frac{q_{CH4}^{CE}}{q_{CH4}^{ST}} - 1\right)$ *External (%)*
9.09	10	4.90	10	5.63	10.2	4.49	9.16	25.31
9.09	30	13.83	30	13.84	30.2	10.16	36.12	36.22
9.09	60	24.42	60	24.45	60.3	16.37	49.16	49.36
5.13	10	52.20	10	52.81	10.2	45.69	14.24	15.56
5.13	20	10.17	20	10.19	–	–	–	–
5.13	32.8	13.26	30	13.65	30.2	10.23	29.61	33.44
5.13	40	17.12	40.1	17.14	–	–	–	–
5.13	60	24.18	60	24.22	–	–	–	–
1.14	10	52.33	10.8	5.25	–	–	–	–
1.14	30	12.71	30	12.79	–	–	–	–
1.14	60	21.30	60	21.51	–	–	–	–

Adsorbed amounts. *Conditions* coaxial and single tank systems, stored gas methane, adsorbent activated carbono ($m_{AC} = 132$ g)

Table 3 Comparative evaluation for the storage systems

Flow rate ($Lmin^{-1}$)	Internal cylinder		External cylinder		Single tank		Volume storage increase in the coaxial system	
	P (bar)	$Q_{V/V}^{IC}$ (m^3m-^{3})	P (bar)	$Q_{V/V}^{EC}$ (m^3m^{-3})	P (bar)	$Q_{V/V}^{ST}$ (m^3m^{-3})	$\left(\frac{Q_{V/V}^{IC}}{Q_{V/V}^{ST}} - 1\right)$ *Internal (%)*	$\left(\frac{Q_{V/V}^{EC}}{Q_{V/V}^{ST}} - 1\right)$ *External (%)*
9.09	10	31.70	10	38.08	10.2	29.95	5.84	27.15
9.09	30	92.42	30	92.34	30.2	75.34	22.67	22.56
9.09	60	172.93	60	173.04	60.3	135.49	27.63	27.71
5.13	10	33.19	10	33.52	10.2	30.42	9.11	10.19
5.13	20	65.46	20	65.50	–	–	–	–
5.13	30	89.52	30	91.58	30.2	75.66	18.32	21.04
5.13	40	116.37	40.1	115.85	–	–	–	–
5.13	60	171.34	60	172.18	–	–	–	–

Volumetric estorage capacities. *Conditions* coaxial and single tank systems, stored gas methane, adsorbent activated carbono ($m_{AC} = 132$ g)

system, a larger amount of gas was fed into the coaxial system to achieve the charge pressure, resulting in a greater mass of gas adsorbed, indicating an increase of about 50 % by weight of methane stored at 60 bar. It was estimated that the volumetric storage capacity of the coaxial system was 27.15 % higher than that obtained with the traditional system.

4 Conclusions

A new gas storage system was developed consisting of two coaxial cylinders filled with an equal mass of a porous activated carbon (1634 m^2/g, Nuchar NG, West Med Vacuum USA). The coaxial system storage capacity was evaluated using the ANG process operating in cycles involving compression and adsorption in the internal cylinder, and simultaneous decompression and desorption in the external cylinder.

The combination of heat exchange between the storage tanks, mainly due to the adsorption and desorption, was effective for maintaining the equilibrium temperature between 24 and 26° C.

In comparison with the traditional system, the coaxial system was able to store a greater mass of gas. An increase of about 50 % by weight of methane was stored under 60 bar, which corresponds to a 27.15 % higher volumetric storage capacity.

Acknowledgments We would like to acknowledge PPEQ/UFPE and CNPq, Brazil for the financial support to this project.

References

Basumatary, R., Dutta, P., Prasad, M., Srinivasan, K.: Thermal modeling of activated carbon based adsorptive natural gas storage system. Carbon **43**, 541–549 (2005)

Bastos-Neto, M., Torres, A.E.B., Azevedo, D.C.S., Cavalcante, C.L.: A theoretical and experimental study of charge and discharge cycles in a storage vessel for adsorbed natural gas. Adsorption **11**, 147–157 (2005)

Biloé, S., Goetz, V., Mauran, S.: Dynamic discharge and performance of a new adsorbent for natural gas storage. AIChE J. **47**(12), 2819–2830 (2001)

Chang, K.J., Talu, O.: Behavior and experimental performance of adsorptive natural gas storage cylinders during discharge. Appl. Therm. Eng. **16**(5), 359–374 (1996)

Do, D.D.: Dynamics of a semi-batch adsorber with constant molar supply rate: a method for studying adsorption rate of pure gases. Chem. Eng. Sci. **50**(3), 549–553 (1995)

Gadipelli, S., Guo, Z.X.: Graphene-based materials: synthesis and gas sorption, storage and separation. Prog. Mater. Sci. **69**, 1–60 (2015)

Hirata, S.C., Couto, P., Larac, L.G., Cotta, R.M.: Modeling and hybrid simulation of slow discharge process of adsorbed methane tanks. Int. J. Therm. Sci. **48**(6), 1176–1183 (2009)

Lozano-Castelló, D.D., Linares-Solano, A., Quinn, D.F.: Influence of pore size distribution on methane storage at relative low pressure: preparation of activated carbon with optimum pore size. Carbon **40**, 989–1002 (2002)

Mason, J.A., Veenstra, M., Long, J.R.: Evaluating metal–organic frameworks for natural gas storage. Chem. Sci. **5**, 32–51 (2014)

Matranga, K.R., Myers, A.L., Glandt, E.D.: Storage of natural gas by adsorption on activated carbon. Chem. Eng. Sci. **47**(7), 1569–1791 (1992)

Mota, J.P.B.: Impact of gas composition on natural gas storage by adsorption. AIChE J. **45**(5), 986–996 (1999)

Mota, J.P.B., Saatdjian, E., Tondeur, D., Rodrigues, A.E.: A simulation model of a high capacity methane adsorptive storage system. Adsorption **1**, 17–27 (1995)

Prajwal, B.P., Ayappa, K.G.: Evaluating methane storage targets: from powder samples to onboard storage systems. Adsorption **20**(5–6), 769–776 (2014)

Pupier, O., Goetz, V., Fiscal, R.: Effect of cycling operations on an adsorbed natural gas storage. Chem. Eng. Process. **44**, 71–79 (2005)

Reid, R.C., Prausnitz, J.M., Poling, B.E.: The Properties of Gases and Liquids, 4th edn. McGraw-Hill, New York (1987)

Santos, J.C., Marcondes, F., Gurgel, J.M.: Performance analysis of a new tank configuration applied to the natural gas storage systems by adsorption. Appl. Therm. Eng. **29**(11–12), 2365–2372 (2009)

Stritih, U., Bombač, A.: Description and analysis of adsorption heat storage device. J. Mech. Eng. **60**(10), 619–628 (2014)

Vasiliev, L.L., Kanonchik, L., Mishkinis, D., Rabetsky, M.: Adsorbed natural gas storage and transportation vessels. Int. J. Therm. Sci. **39**, 1047–1055 (2000)

Walton, K.S., LeVan, M.D.: Natural gas storage cycles: influence of nonisothermal effects and heavy alkanes. Adsorption **12**(3), 227–235 (2006)

Wegrzyn, J., Gurevich, M.: Adsorbent storage of natural gas. Appl. Energy **55**(2), 71–831 (1996)

Yahia, S.B., Ouederni, A.: Hydrocarbons gas storage on activated carbons. Int. J. Chem. Eng. Appl. **3**(3), 220–227 (2012)

Yang, X.D., Zheng, Q.R., Gu, A.Z., Lu, X.S.: Experimental studies of the performance of adsorbed natural gas storage system during discharge. Appl. Therm. Eng. **25**, 591–601 (2005)